

# Simulations for eROSITA:

## First impressions on the imaging properties



ERLANGEN CENTRE  
FOR ASTROPARTICLE  
PHYSICS



## Bachelorarbeit

Dr. Karl Remeis-Sternwarte Bamberg  
Universität Erlangen - Nürnberg

Hochschule Coburg - university of applied science and arts



**COBURG UNIVERSITY**  
of applied sciences and arts

vorgelegt von: Margarita Behm  
Studienbereich: Technische Physik -  
Licht- und Lasertechnologie  
Matrikelnummer: 00473513  
Erstbetreuer: Prof. Dr. Jörn Wilms  
Zweitbetreuer: Prof. Dr. Wolfram Haupt





## Abstract

This bachelor thesis is about simulations for eROSITA. eROSITA is an X-ray telescope which will be launched in Spring 2018 to study current cosmological models. In the first four years it will perform an all sky survey and therefore scan the whole sky. During that time it is expected to detect 50000 to 100000 new galaxy clusters in the X-ray data. In order to clarify if a new source was detected, simulations are created and the analysis software is tested. That way we get a first impression on the imaging capabilities of eROSITA.

The simulations are roughly designed in such a way that a region in the sky with its known X-ray sources was first implemented, to which further parameters and variables of the sources are added. Since we want to detect new sources with the aid of the telescope, we first must understand how the software generally detects X-ray sources. At the beginning I give some information about eROSITA, X-ray telescopes and the software. An explanation of the simulations and their results follows. Finally, I discuss the outcome of the simulations and give conclusions about their meaning for the eROSITA mission.



## Zusammenfassung

Diese Bachelorarbeit handelt von Simulationen, die für eROSITA durchgeführt wurden. eROSITA ist ein Röntgenteleskop, das voraussichtlich im Frühling 2018 starten wird, um die derzeitigen kosmologischen Modelle zu studieren. In den ersten vier Jahren wird es eine Himmelsuntersuchung durchführen und dazu den kompletten Himmel scannen. In dieser Zeit sollen 50000 bis 100000 neue Galaxienhaufen im Röntgenbereich gefunden werden. Um herauszufinden, ob es sich dabei um neue Quellen handelt, werden die Simulationen erstellt und dabei die Software getestet. Auf diese Weise erhält man einen ersten Eindruck der Abbildungseigenschaften von eROSITA.

Im Groben sind die Simulationen so aufgebaut, dass zuerst eine Region am Himmel mit ihren bekannten Röntgenquellen erzeugt wurde, in die anschließend weitere Parameter und Variablen zu den Quellen hinzugefügt wurden. Da man mit Hilfe des Teleskopes neue Quellen finden will, muss man vorher verstehen, wie die Software Röntgenquellen im Allgemeinen detektiert. Zu Beginn gebe ich ein paar Informationen zu eROSITA, Röntgenteleskopen und der Software. Anschließend folgt eine Erklärung zur Vorgehensweise der Simulationen und deren Ergebnisse. Die Arbeit endet mit einer Diskussion über die Resultate und ihre Bedeutung für die Mission.



# Contents

<b>List of Figures</b>	<b>III</b>
<b>List of Tables</b>	<b>IV</b>
<b>List of Acronyms</b>	<b>V</b>
<b>1. Introduction</b>	<b>1</b>
1.1. Motivation . . . . .	2
1.2. eROSITA . . . . .	3
1.3. Technical details . . . . .	5
<b>2. X-ray telescopes</b>	<b>7</b>
2.1. Optics . . . . .	7
2.2. Detectors . . . . .	11
<b>3. Software</b>	<b>14</b>
3.1. SIXTE . . . . .	14
3.1.1. SIMPUT . . . . .	15
3.1.2. erosim . . . . .	16
3.2. eSASS . . . . .	17
<b>4. Simulation</b>	<b>19</b>
4.1. Simple example . . . . .	19
4.2. Creating the Skymap . . . . .	22
4.3. Andromeda Galaxy aka M31 . . . . .	24
4.3.1. Simput of M31 . . . . .	24
4.3.2. Diffuse emission of M31 . . . . .	25
4.4. Analysing the Skymap . . . . .	28
<b>5. Results</b>	<b>31</b>
<b>6. Conclusion</b>	<b>34</b>



Simulations for eROSITA:  
First impressions on the imaging properties

*Contents*

---

<b>Bibliography</b>	<b>35</b>
<b>Acknowledgements</b>	<b>37</b>
<b>Eidesstattliche Erklärung</b>	<b>38</b>
<b>A. Appendix</b>	<b>i</b>



## List of Figures

1.1. SRG-satellite with both instruments . . . . .	1
1.2. Second Lagrangian point . . . . .	4
1.3. Scanning Attitude of eROSITA . . . . .	4
1.4. Image of the 4-year all sky survey . . . . .	5
2.1. Wolter type I telescope . . . . .	8
2.2. ARF of eROSITA . . . . .	10
2.3. eROSITA's vignetting function . . . . .	11
2.4. Schematic CCD of eROSITA with readout . . . . .	13
3.1. Schematic layout of a simulation pipeline . . . . .	15
4.1. Difference of slew survey and pointed observation . . . . .	21
4.2. First simulation with just the <code>rass.simput</code> . . . . .	23
4.3. Second simulation adding the AGN population . . . . .	23
4.4. Third simulation adding the light curve . . . . .	23
4.5. Fouth simulation with adding M31 . . . . .	25
4.6. Mosaic picture of the Andromeda Galaxy . . . . .	26
4.7. Cut out sources of the Andromeda Galaxy . . . . .	27
4.8. Diffuse emission of the Andromeda Galaxy . . . . .	27
4.9. The simulation with the diffuse emission of M31 . . . . .	28
4.10. Energy band 1 and 2 . . . . .	29
4.11. Energy band 3 and 4 . . . . .	29
5.1. Source map 1 and 2 . . . . .	32
5.2. Source map 3 and 4 . . . . .	32
A.1. Energy bands in another colour . . . . .	i
A.2. Source maps in another colour . . . . .	ii



## List of Tables

1.1. eROSITA's specifications . . . . .	6
3.1. Specification of important SRC_CAT data . . . . .	15
3.2. Parameters for erosim . . . . .	16





## List of Acronyms

<b>ABRIXAS</b>	<i>A Broadband Imaging X-ray All-Sky Survey</i>
<b>AGN</b>	<i>Active Galactic Nucleus</i>
<b>ARF</b>	<i>Ancillary Response File</i>
<b>ART-XT</b>	<i>Astronomical Roentgen Telescope – X-ray Concentrator</i>
<b>CCD</b>	<i>Charge-Coupled Device</i>
<b>Dec</b>	<i>Declination</i>
<b>eROSITA</b>	<i>extended ROentgen Survey with an Imaging Telescope Array</i>
<b>eSASS</b>	<i>extended Science Analysis Software System</i>
<b>FOV</b>	<i>Field Of View</i>
<b>HDU</b>	<i>Head and Data Unit</i>
<b>HEW</b>	<i>Half Energy Width</i>
<b>OOT</b>	<i>Out Of Time</i>
<b>PDF</b>	<i>Probability Density Function</i>
<b>PSD</b>	<i>Power Spectral Density</i>
<b>PSF</b>	<i>Point Spread Function</i>
<b>RA</b>	<i>Right Ascension</i>
<b>RASS</b>	<i>ROSAT all sky survey</i>
<b>RMF</b>	<i>Redistribution Matrix File</i>
<b>ROSAT</b>	<i>ROentgen SATellite</i>
<b>SIMPUT</b>	<i>SIMulation inPUT</i>
<b>SIXTE</b>	<i>SIMulation of X-ray TElescopes</i>
<b>SNR</b>	<i>SuperNova Remnant</i>
<b>SRG</b>	<i>Spectrum-Roentgen-Gamma</i>
<b>ULX</b>	<i>ultra-luminous X-ray source</i>
<b>XMM-Newton</b>	<i>X-ray Multi-Mirror Newton</i>





## 1. Introduction

eROSITA is an abbreviation for extended Roentgen Survey with an Imaging Telescope Array. It is an X-ray telescope and together with the Russian Astronomical Roentgen Telescope–X-ray Concentrator (ART-XC) it will be launched in Spring 2018 from Baikonur, Kazakhstan, aboard the Russian Spektrum–Roentgen–Gamma satellite (SRG, Fig. 1.1). Altogether there are eight German institutes developing eROSITA, one of them is the Remeis-Sternwarte in Bamberg.

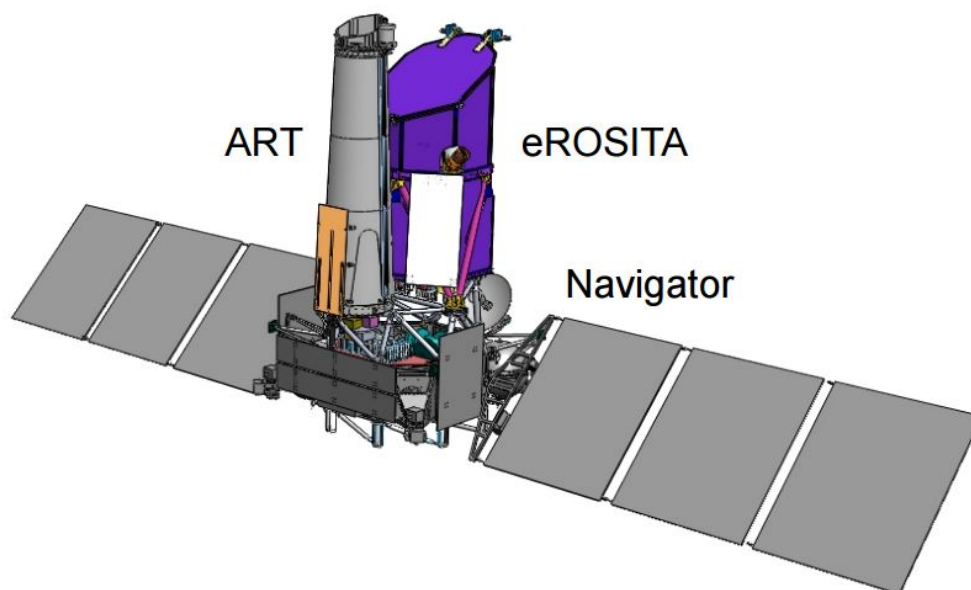


Figure 1.1.: SRG with ART-XC and eROSITA on its Navigator platform (taken from Predehl, 2010)



## 1.1. Motivation

Although we know much about the current cosmological model, there are still things we have to understand, e.g., the nature of the Dark Energy and Dark Matter. It is hard to describe what Dark Energy and Dark Matter is since we know like nothing about it. What we know is that about 68% of the universe are made of Dark Energy and roughly 27% of Dark Matter. Only about 5% are the so called Baryonic Matter, the common matter, which we have understood and can explain due to observations.<sup>1</sup>

We can be sure of the existence of Dark Matter although we are not able to see or detect it with our current instruments. The reason for that is the strange behavior of stars at the edge of a spinning spiral galaxy. Usually one can imagine that a star at the edge would orbit the galactic center at a much slower speed than one near it. This is the standard physics we all learned in school.

$$v = \sqrt{G \cdot M \cdot \left(\frac{2}{r} - \frac{1}{a}\right)} \quad (1.1)$$

where  $G$  is the gravitational constant,  $M$  is the mass,  $r$  is the distance and  $a$  is the large semi-axis. But observations have shown that it does not matter where a star is located, since they all move at approximately the same speed around their center.<sup>2</sup> That means in turn that there must be something that explains this cohesion among the stars and this is what we call Dark Matter.

Dark Energy, on the other hand, is even more mysterious. Knowing Big Bang Theory (not the TV-show) physicists assumed that the universe would expand slower over time due to the attractive force of gravity.<sup>1.1</sup> It was a shock when an “*accelerating expansion of the Universe*”<sup>3</sup> was discovered back in the 1990s leading to a nobel prize in 2011 by the way. The physics behind this phenomenon is the Dark Energy.

One of the goals of eROSITA is to give us a better understanding of Dark Energy and Dark Matter. To reach this goal the telescope will do a four year all sky survey and detect 50000 to 100000 galaxy clusters which can be detected by emitting in X-rays due to their hot gas in the center (Merloni et al., 2012).

---

<sup>1</sup><https://science.nasa.gov/astrophysics/focus-areas/what-is-dark-energy>

<sup>2</sup><http://science.nationalgeographic.com/science/space/dark-matter/>

<sup>3</sup>[https://www.nobelprize.org/nobel\\_prizes/physics/laureates/2011/press.html](https://www.nobelprize.org/nobel_prizes/physics/laureates/2011/press.html)

# Simulations for eROSITA:

First impressions on the imaging properties



## 1. Introduction

---

Another goal is to study black holes and their evolution. This can be done by comparing nearby (i.e., young) and distant (i.e., old) Active Galactic Nuclei (AGNs). It is believed that in the center of each AGN there is a massive black hole.<sup>4</sup> eROSITA is predicted to detect 3 to 10 million AGNs (Merloni et al., 2012). In those first four years, eROSITA is also going to find supernova remnants (SNRs), neutron stars, and other X-ray binary systems. By observing the dust scattering halos, new information will be obtained about the chemical composition of interstellar dust (Merloni et al., 2012). But in order to detect all of those objects, the sensitivity of eROSITA had to be improved compared to ROSAT. ROSAT (Roentgen Satellite), which started its all sky survey in 1990 and ended it eight years later (Voges et al., 1999), was the predecessor of eROSITA. eROSITA's sensitivity will be twenty times more sensitive in the soft X-ray band (0.5–2 keV). Also eROSITA will provide the first imaging survey of the sky in the hard band (2–10 keV). A more detailed specification of eROSITA is given in depth by Merloni et al. (2012) and references therein.

## 1.2. eROSITA

eROSITA will be orbiting with the Earth-Sun system around the second Lagrangian point  $L_2$  (Fig. 1.2). The second Lagrangian point is 1.5 million km behind the Earth in the anti-Sun direction. At this position the satellite will be far enough away from Earth to avoid its heat radiation and it allows a longer and stable observation. To avoid reorienting the solar panels too often, the satellite rotates around an axis, which points towards the sun with a small offset. In the first four years of the mission, eROSITA will perform an all sky survey. It will scan the sky over a  $1^\circ$  wide stripe by rotating around its axis with one revolution per four hours (Fig. 1.3). This four hour survey is called an eROSITA day (eroday). The poles of the survey are positioned at about RA =  $270.00^\circ$  and Dec =  $66.20^\circ$  and at about RA =  $90.00^\circ$  and Dec =  $-66.20^\circ$ . They will be scanned more often, resulting in a deeper exposure in that area compared to the region of the survey equator.

During the four year all sky survey, each region in the sky will be revisited at least eight times. Figure 1.4 shows a visualization of the position-dependent effective exposure time after four years using a logarithmic intensity scale. The

---

<sup>4</sup><https://heasarc.gsfc.nasa.gov/docs/objects/agn/agn.txt.html>

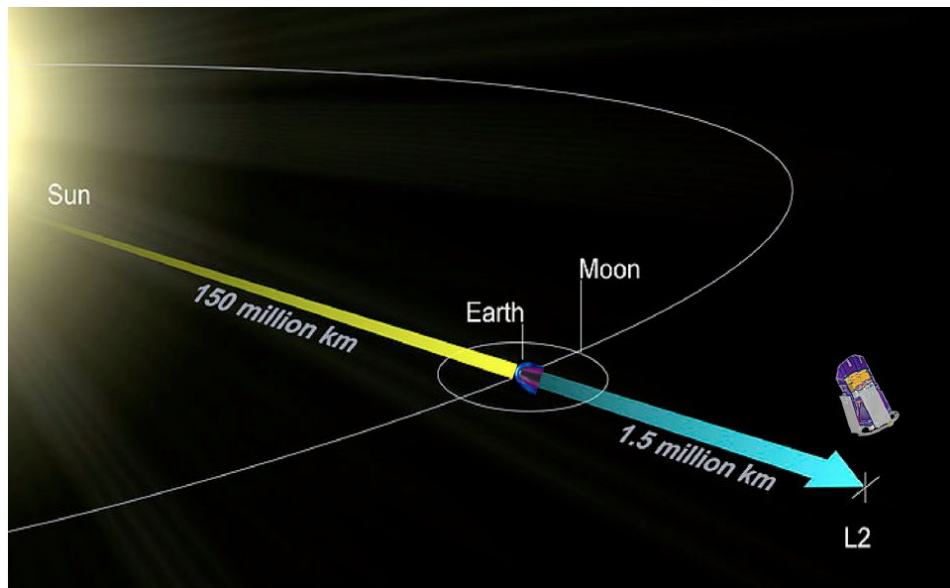


Figure 1.2.:  $L_2$  is located 1.5 million km behind the Earth in the anti-Sun direction (taken from Merloni et al., 2012)

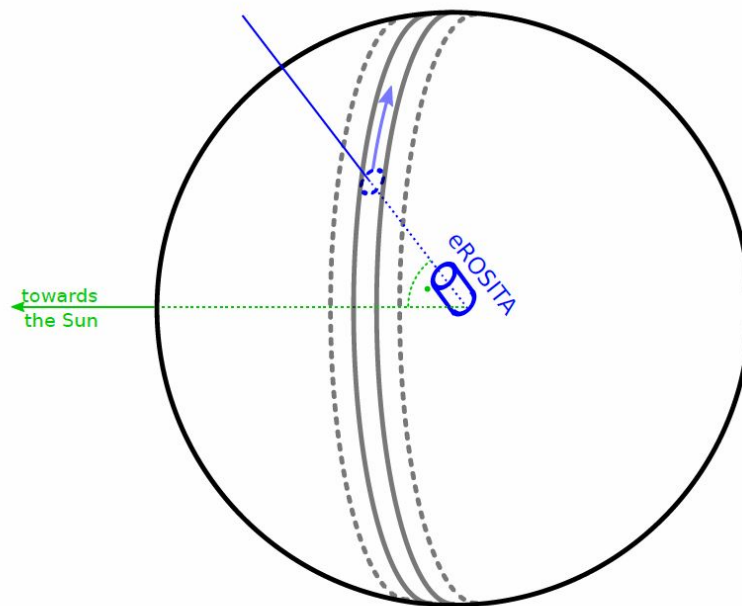


Figure 1.3.: eROSITA's scanning attitude for the sky (taken from Schmid, 2012)

bright spots are as mentioned before the ecliptic poles. The brighter a region is the more exposure time is spent in it. After that it is planned for eROSITA to perform a pointed observation lasting about three years.

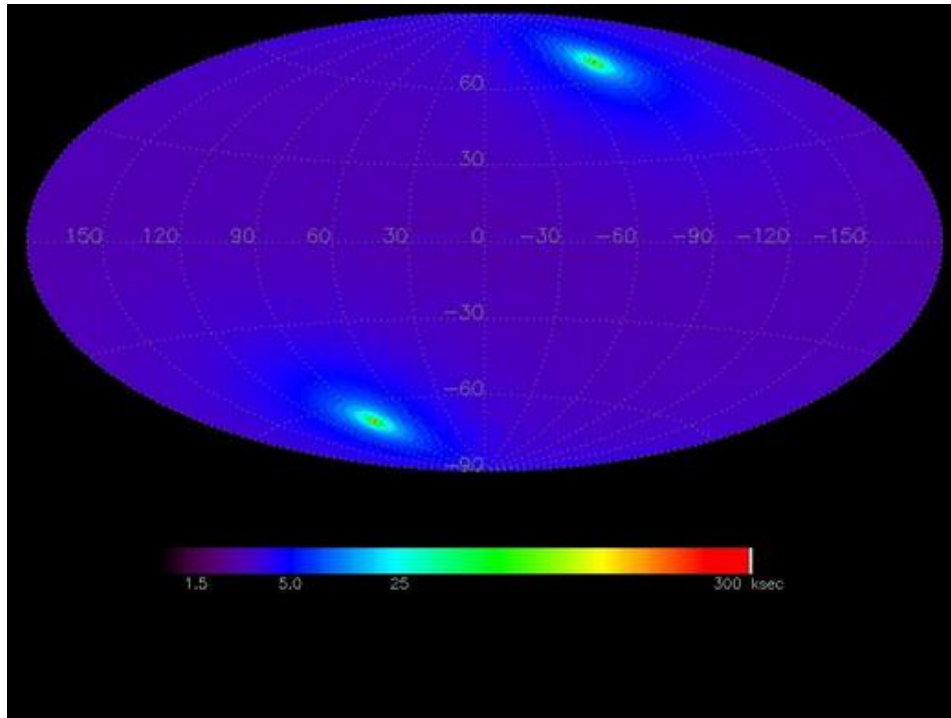


Figure 1.4.: Image of the position dependent effective exposure time of the 4-year eROSITA all sky survey scaled logarithmic, based on the current mission scenario (<http://www.mpe.mpg.de/455799/instrument>)

### 1.3. Technical details

The eROSITA instrument consists of seven telescopes in a hexagonal arrangement which are looking in the same direction and are positioned almost perpendicular on the spacecraft platform. These telescopes are similar to the ones of ABRIXAS (A Broadband Imaging X-ray All-Sky Survey), which could never be used in scientific studies. They consist of seven Wolter type I mirror modules (Wolter, 1952). An X-ray baffle placed in front of them to reduce the amount of stray photons. Each of these mirror modules consists of 54 mirror shells with an outer diameter of 360 mm. In order to operate independently, each mirror module has its own detector. The advantages of that multiple mirror systems are a shorter focal length and a reduced pile up while observing bright sources (see Section 2.2 below). Another reason is multiple redundancy: the mission can still go on even if one or more instruments are malfunctioning. The focal length of each telescope is 1600 mm.



Table 1.1.: Specifications of the eROSITA telescope

telescope type	7 Wolter-I mirror shells
mirror shells per module	54
diameter of each mirror shell	360 mm
focal length	1600 mm
detector type	frame-store pn-CCD
detector pixels	$384 \times 384$
size of pixels	$75 \times 75 \mu\text{m}$
FOV	61 arcmin
on-axis resolution	15 arcsec at 1keV
energy range	0.2 - 10 keV
energy resolution	$\sim 130$ keV
time resolution	50 ms

eROSITA is sensitive from 0.2 keV up to 10 keV. At 6 keV it has an energy resolution of around 130 keV. The telescopes have a field of view (FOV) with a diameter of 61'. Due to the geometry and the mirror properties, the spatial resolution depends on the energy and the off-axis angle. The resolution at 1 keV is 15 arcsec and over the entire FOV about 26–30 arcsec. The pn-CCD detector inside of each sub-telescope consists of two parts. The first one is an X-ray sensitive imaging area with  $384 \times 384$  pixels covering an area of  $28.8 \text{ mm} \times 28.8 \text{ mm}$  and a size per pixel of  $75 \mu\text{m} \times 75 \mu\text{m}$  to measure incoming X-ray photons. The other region is a frame-store area with the same number. This region is shielded against X-rays. While observing the sky the imaging area is exposed to incident photons. Every 50 ms the collected charges are shifted into the frame-store area. Here they can be read out without confusion by further incident photons. This way out of time (OOT) events can be avoided.





## 2. X-ray telescopes

X-ray sources, as the name suggests, emit light in X-rays and are therefore not visible in the optical, but at wavelength from around  $10^{-9}$  m to  $10^{-11}$  m (corresponding to 0.1–10 keV). In order to detect those photons, due to the low fluxes, eROSITA must have some sort of collecting optics.

### 2.1. Optics

Usually imaging with an optical telescope is done by refraction or reflection. Refraction is described in the law of Snellius,

$$\frac{\sin(\alpha)}{\sin(\beta)} = \frac{n_2}{n_1} \quad (2.1)$$

Light will always be refracted at the transition from a medium with refraction index  $n_1$  to another medium with refraction index  $n_2$ .  $\alpha$  is the angle of the incoming photons from the normal of the border between the two media, whereas  $\beta$  is the angle of the refracted photons. If the angle of the incoming photons is bigger than the critical angle  $\gamma_c$  total reflection occurs,

$$\gamma_c = \arcsin\left(\frac{n_2}{n_1}\right) \quad (2.2)$$

Since the Earth's atmosphere absorbs UV, X-rays and  $\gamma$ -rays it is only possible to observe the sky in the visible spectra from the Earth (Seward & Charles, 2010). Therefore X-ray telescopes are mounted on satellites orbiting Earth. The index of  $n_1 = 1$  due to the vacuum in space. The refraction index  $n_2$  is slightly less than unity for matter at X-ray wavelengths (Aschenbach, 1985, 2009) such that  $\gamma_c$  is around  $90^\circ$ . This circumstance makes it hard for photons to be reflected because they have to incidence under a very flat angle. This also means that refraction is difficult because of  $\alpha \approx \beta$ .

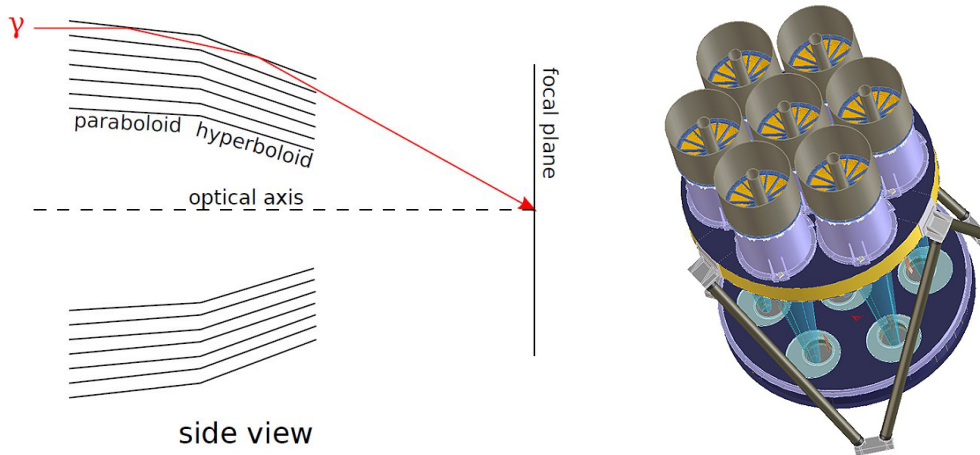


Figure 2.1.: Left: A drawing of the Wolter type I X-ray telescope. An incident photon will be double-reflected on the paraboloid and hyperboloid surface and focused on a single spot in the focal plane (taken from Schmid, 2012)  
Right: eROSITA with its seven Wolter type I telescopes ([http://www.dlr.de/rd/desktopdefault.aspx/tabid-2448/3635\\_read-24151/](http://www.dlr.de/rd/desktopdefault.aspx/tabid-2448/3635_read-24151/))

Therefore optical telescope designs, where radiation arrives almost perpendicular to the optical surfaces, are not applicable for X-rays and new techniques had to be developed. One possible solution is to use coded masks in front of a position sensitive detector, such as to block incoming photons in some areas. Due to knowing the mask, reconstruction of the incident photons is possible based on the measurements of the detector (Schmid, 2012). An alternative are focusing optics. In 1952 Wolter designed three different telescope models for X-rays which use total reflection (Wolter-I, Wolter-II and Wolter-III). The multiple mirrors were arranged to fulfill Abbé's sine condition,

$$\frac{h}{\sin(\phi)} = f \quad (2.3)$$

where  $h$  is the distance between target and optical axis,  $\phi$  is the angle between the refracted beam and optical axis and  $f$  is the focal length. Wolter-I telescopes as used on eROSITA consist of a combination of paraboloid and hyperboloid surface in order to reflect a photon more than once (Trümper & Hasinger, 2008). Each of these seven telescopes consists of 54 nested mirrors to increase the effective area. This way an incident photon will be double-reflected on the surface of the mirror and focused on the focal point (Trümper & Hasinger, 2008). There are different properties characterizing an imaging X-ray telescope, beginning

# Simulations for eROSITA:

## First impressions on the imaging properties



### 2. X-ray telescopes

---

with the Field of View (FOV). It specifies which angular area is covered by the optics, but only in a very rough approximation. Since the optical properties worsen by the boundaries of the FOV and due to the limitations of the optical systems, it is possible to measure photons coming from outside the FOV. These limitations are set by the strong astigmatism of the Wolter telescopes, which can not be manufactured in a better way. The result is that these photons degrade the imaging quality. The degradation can be avoided by collimating baffles in front of each mirror shell. The other three properties are: the effective area, the vignetting function, and the Point Spread Function (PSF). The effective area describes the energy dependency of the optical system and the detectors. It is the product of the projected area of the optics and the reflectivity of the mirrors, defined as the ratio of the incoming and reflected photons, and often also include terms which take into account the sensitivity of the detectors. The effective area is commonly stored in an Ancillary Response File (ARF, Fig. 2.2), which contains the sensitivity of the instrument in dependence of the energy, as specified by George et al. (2007). For an X-ray mission a large effective area is essential for detecting very faint sources. The vignetting function describes the probability that photons reach the detector. A function of the off-axis angle, the azimuthal angle, and the photon's energy. Since the vignetting function is zero outside the FOV, photons from there will be rejected. Considering the off-axis and the azimuthal angles as well as the energy of a photon the vignetting function characterizes the probability that a photon is hitting the surface of the detector. In other words the vignetting function is the probability that a photon hits the detector. Figure 2.3 shows the vignetting function for different energies of the photons. Ideally it would be units over the entire FOV, but in reality not all photons inside the FOV hit the surface of the detector. The Point Spread Function describes the imaging capabilities of an X-ray telescope. More precisely it depicts the image of an observed on-axis, point-like source on the detector. The corresponding distribution on the detector  $D(x, y)$  for a given distribution for incident photons  $I(x, y)$  is given by the convolution of  $I$  and the PSF,

$$D(x, y) = (I \cdot \text{PSF})(x, y) = \int_{-\infty}^{\infty} dx' \int_{-\infty}^{\infty} I(x', y') \cdot v(x', y') \cdot \text{PSF}(x-x', y-y') dy' \quad (2.4)$$

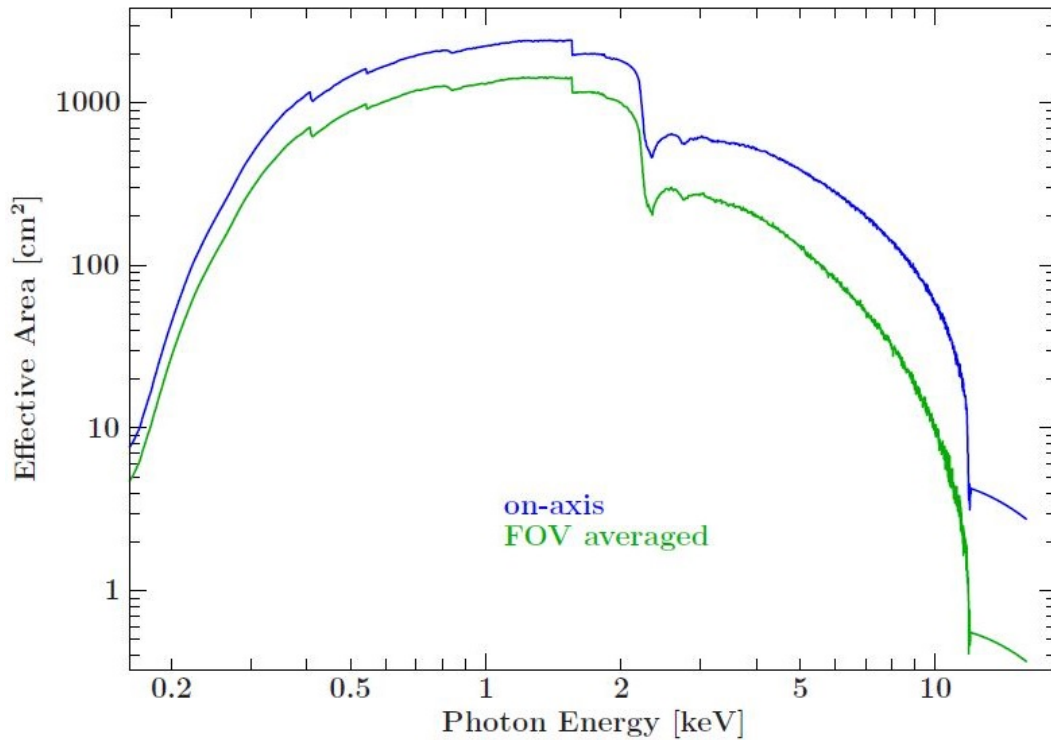


Figure 2.2.: The ARF of eROSITA. The blue curve is for an observation on the optical axis, the green one is the mean value over the entire FOV (taken from Schmid, 2012)

The PSF depends on the energy of the photons. It is necessary to regularly include off-axis incoming photons, which means to add more parameters, but the keynotes of the PSF remain. By the way the parameters used here are Cartesian coordinates, but they can be easily transformed to polar coordinates. To calculate the angular resolution at Half Energy Width (HEW) the PSF is used,

$$\int_0^{\frac{HEW}{2}} dr \int_0^{2\pi} r \cdot \text{PSF}(r, \varphi) d\varphi = \frac{1}{2} \quad (2.5)$$

It is understood as the diameter of the circle in which 50% of the incoming photons are at the focus (Schmid, 2012). In reality a PSF is rather complicated, especially for the optics of eROSITA.

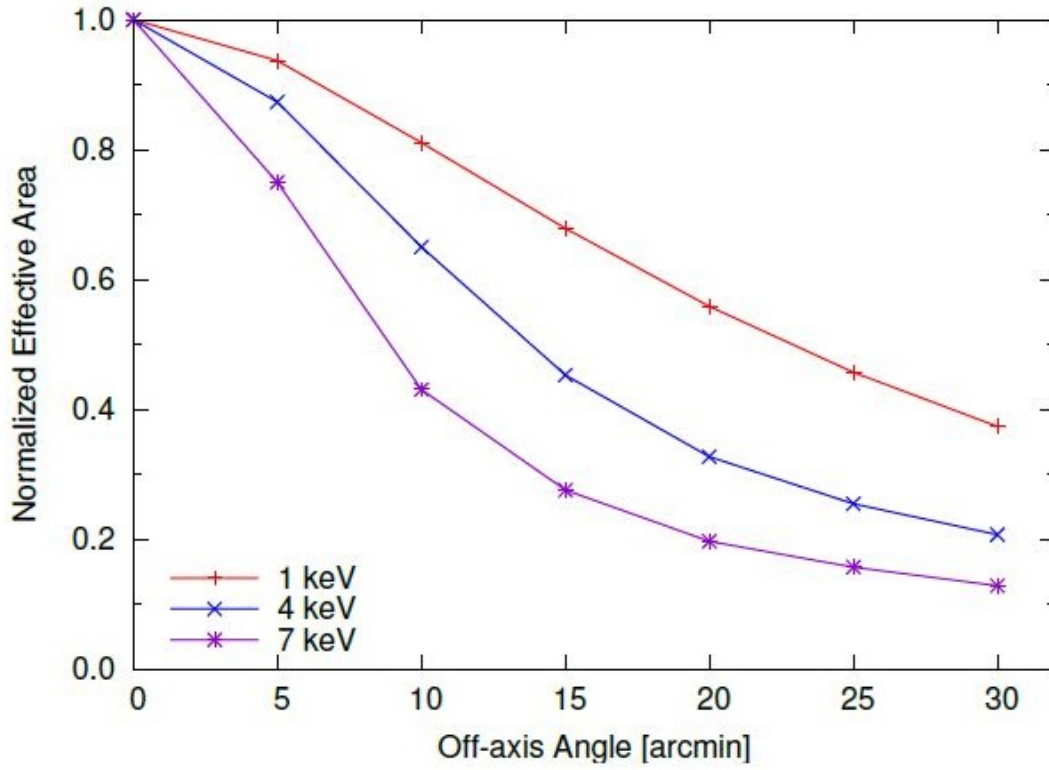


Figure 2.3.: The vignetting function of eROSITA for different energies (taken from Schmid, 2012)

## 2.2. Detectors

eROSITA is using Charge-Coupled Devices (CCDs) as detectors. Due to their good spatial resolution, CCDs are the best way to perform imaging in the X-ray astronomy. In X-ray astronomy it is possible to detect individual photons because the photon energies are high enough and the rates are low enough (Lumb et al., 1991). For photons with an energy below 50 keV the photoelectric absorption is the dominant interaction mechanism (Schmid, 2012). The energy to excite an electron into the conduction band is a few eV. This means that for optical light, an average photon excites an electron into the conduction band. In X-rays, however, photons have a higher energy of a few 1000 eV. The consequence are inelastic collisions of the photoelectrons released after absorption with other photons in the valence band. The result is an amount of electrons in the conduction band of

$$N = \frac{h\nu}{E_{\text{gap}}} = \frac{E}{E_{\text{gap}}} \quad (2.6)$$



with  $E_{\text{gap}}$  about 1.8 eV for silicon. Thus the charges measured in the pixels are proportional to the energy of the invaded photons. Considering the Poisson effect with an uncertainty of

$$\frac{\Delta E}{E} = 2.335 \sqrt{\frac{3.65 \text{ eV} \cdot F}{E}} \quad (2.7)$$

with  $F \sim 0.1$  means  $\sim 2\%$  at 5.9 keV which is actually much better than proportional counters (Wilms, 2017). The factor  $F$  is a correct for the fact that the absorption is not fully stochastic. When a photon hits a pixel, electron-hole pairs are created. The generated charges are then trapped in an electric field. By shifting the charges from one to another pixel, all pixels in one row of the CCD can be read out. At the end of one line is a readout buffer. This process is illustrated in Fig. 2.4. In the eROSITA CCDs the exposure time is 50 ms, while the readout process take a few  $\mu\text{s}$  (Meidinger et al., 2009). It stores temporary the charges which fall out of the array due to the shifting, where they can be measured by using Analogue/Digital converter (Kartunen et al., 2003). Although CCDs have a lot of advantages like the small size and low weight, they also can lead to some problems. A more detailed explanation of these effections is given by Schmid (2012) or Wille (2011).

**Blooming:** The potential wells are limited and can therefore only hold a certain amount of charge. If the exposure time is too long electrons can overflow into neighbouring pixels and by that making the data useless.

**Out of time (OOT) events:** As mentioned in Section 1.3, OOT events occur when photons hit the CCD during the readout process. The consequence is that it is impossible to interpret the incoming photons correctly. To avoid OOT events a frame-store area in the CCD is used to store the charges temporarily.

**Split events:** When an incoming photon impacts near the boundary of one pixel the resulting charge will be collected in more than one pixel. Although a thin insulating layer is placed between the columns it is not sufficient enough to avoid the split events.

**Pile up:** To reconstruct the energy of one photon which had an impact on the detector it has to be distinguishable from the other photons. In other words it is impossible to separate one photon with a certain energy of several photons with the sum of the same energy.



## 2. X-ray telescopes

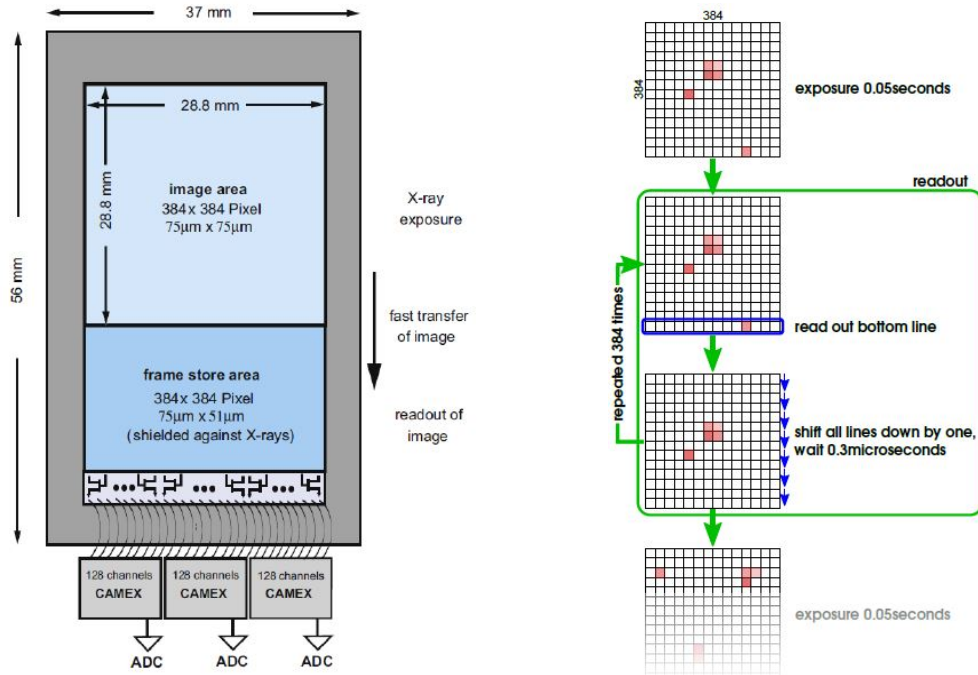


Figure 2.4.: Left: Illustration of a CCD of eROSITA. Incident photons create charges in the pixels of the image area (Meidinger et al., 2009). After an exposure of 50 ms the charges are shifted to the frame-store area to be readout as to be seen in the right picture (taken from Brand et al., 2016)

**Dark current:** Due to dark current the data quality is reduced by adding noise to the output signal. To keep this effect as low as possible the temperature has to be low.

**Particle background:** The CCDs can measure not only photons, but also background particles, which could come from solar wind or cosmic rays. This leads again to a worsening of the signal quality.

By using an ARF and a Redistribution Matrix File (RMF) the detector response can be modeled (George et al., 2007). The RMF describes the redistribution by the detector of the incident spectrum's energies. Thus it is possible to calculate the expected value for the counts  $C(h)$  of a particular channel  $h$ ,

$$C(h) = \iint \text{RMF}(h, E) \cdot \text{ARF}(E) \cdot N_{\text{ph}}(E, t) dE dt \quad (2.8)$$

with  $N_{\text{ph}}$  being the rate of photons arriving at the detector.





## 3. Software

After giving some information about eROSTIA and X-ray telescopes, it is time to begin with the software which is used for the simulations. For my simulations I used two different software. The first one is the simulation package Simulation of X-ray Telescopes (SIXTE).<sup>5</sup> It is used to simulate eROSITA's all sky survey. The second one is the extended Science Analysis Software System (eSASS), the dedicated analysis software for eROSITA. It is analysing the results of a simulation (Grossberger, 2014). Both software packages contain a large number of tools, of which I will only explain the ones I have used.

### 3.1. SIXTE

SIXTE is a software package developed to generate mission-independent Monte Carlo simulations for astronomical X-ray instrumentations (Schmid, 2012). The main essential elements are the imaging module and the detector module. The first one is responsible for the modelling of the X-ray optics, the second one can be adjusted for different instrument designs. Furthermore there are more additional auxiliary tools. The key task of SIXTE is to create a photon list wherein each incoming photon is listed with its position, energy and arriving time. The software attempts to model the real measured process as precise as possible. A schematic layout of a simulation pipeline is shown in Fig 3.1. In the first step, a number of photons are generated from a source. After that, these photons pass the representative optics and create an impact list. In the third and last step, the impacts cause a signal in the virtual model of the detector, which leads to an output of an event list after a complex readout behavior (Brand et al., 2016). SIXTE generates seven event lists for eROSITA, one for each telescope module. But in order to do that SIXTE must be fed with data. This necessary information of the sources is assured by the SIMPUT which is

---

<sup>5</sup>[http://www.sternwarte.uni-erlangen.de/research/sixte/data/simulator\\_manual\\_v1.1.pdf](http://www.sternwarte.uni-erlangen.de/research/sixte/data/simulator_manual_v1.1.pdf)



# Simulations for eROSITA:

First impressions on the imaging properties



## 3. Software

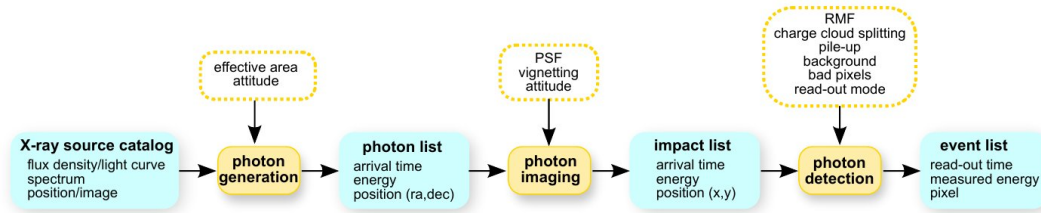


Figure 3.1.: This is what a simulation pipeline looks like schematically to create an event list (taken from Schmid, 2012).

Table 3.1.: Important specifications of the source catalog for the SIMPUT in order to properly perform a realistic simulation

Source ID	the ID of each source
Source Name	apart from the source ID, the corresponding name is also mentioned
RA, Dec	the position of each source given in the equatorial coordinate system
Flux	flux emission of the source in a specified energy band
$E_{\min}$ , $E_{\max}$	defines the borders of a given flux
SPECTRUM	gives a link to the corresponding spectrum which is stored in a different HDU
TIMING	links each source to its light curve in a different HDU if its flux varies with time

specifying the simulation input. More information about SIXTE are available on the web.

### 3.1.1. SIMPUT

SIMPUT is the short form of simulation input and contains all needed information for the simulations in a catalog (Schmid et al., 2013). Its file format is based on the FITS standard (Hanisch et al., 2001; Pence et al., 2010) which is commonly used in astronomy. The data in the file are provided, e.g., by previous missions. Due to an instrument-independent definition of sources the SIMPUT file can be used for simulations of different instruments. The SIMPUT consists of a table with different Header and Data Units (HDUs). Its core extension is the source catalog called SRC\_CAT. This is where the sources are characterized by position, energy or observed flux. The most important specifications can be seen in Table 3.1. For the SIMPUT file the spectrum is obligatory. There are two different ways to describe the energy spectrum of a source. The first one is



Table 3.2.: This are the most important parameters for the tool erosim. The parameters can be adapted for the requested simulation

XMLFile	XML input file with instrument definition for sub-instrument 1-7
Attitude	attitude input file (overwrites RA and Dec)
RA	right ascension of telescope pointing (degree)
Dec	declination of telescope pointing (degree)
Simput	SIMPOT catalog
MJDREF	reference Modified Julian Date
Exposure	exposure time (s)
GTIFile	GTI input file (overwrites TSTART and Exposure)

the mission-independent way by giving a photon flux density in a particular energy range. This method is the most common one. The second way is to give a photon list with the photon energy and arriving time. Usually timing input is optional unless you model a source which is time variable. To simulate a light curve for modelling a brightness variability over time for the sources, one can choose between an explicit light curve or a PSD (Power Spectral Density). The explicit light curve describes the time-dependence of an observed source. On the other hand a PSD, which is the square of the Fourier transformation of the light curve, can be used to characterize stochastic brightness variations.

### 3.1.2. erosim

Apart from the SIMPUT SIXTE needs even more data to perform the simulations for the eROSITA all sky survey with all seven telescope models. The software tool erosim is the one that has to be used for this task. Tab. 3.2 shows the additional needed parameters for that procedure.

**XMLFile:** In the XMLFile many essential parameters of the telescope and detector are defined, such as the FOV diameter, the focal length, the ARF and RMF, the PSF, the pixel size and so on. In other words the XMLFile describes the behaviour of the telescopes. There are seven XMLFiles, i.e., one for each sub-instrument.

**Attitude:** As mentioned before eROSITA will perform an all sky survey and therefore rotate around its axis. This means that with increasing time eROSITA will look at different positions in the sky. The Attitude file specifies at what location eROSITA is looking at a certain time. Without an Attitude file SIXTE

## Simulations for eROSITA:

First impressions on the imaging properties



### 3. Software

---

will simulate a pointed observation which means looking at a certain location in the sky for a given exposure time.

**RA and Dec:** These parts are the Right Ascension and Declination, a system of coordinates used in astronomy, similar to longitude and latitude on Earth (Calabretta & Greisen, 2002). eROSITA will perform a pointed observation with given RA and Dec coordinates. RA and Dec will be ignored if an Attitude is given.

**SIMPOT:** As explained in Sec. 3.1.1, the SIMPUT file contains the most important data like the Source\_ID, Name of the source, Position, Light curve, Spectrum and so on.

**MJDREF:** These letters are understood as reference Modified Julian Date a continuous time scale used in astronomy. A fixed number has been assigned to this parameter.

**Exposure:** The Exposure is the time given in seconds in which eROSITA is performing its simulation. The maximum exposure is 126230400 sec, corresponding to the duration of the four year all sky survey. Since the Exposure always starts at 0 and ends with the given value, you can also specify a START and STOP time instead.

**GTIFile:** The GTIFile is the short form of Good Time Interval and is similar to the START and STOP parameter, as it contains a list of START and STOP times. In combination with the attitude file eROSITA will look in a certain direction given by the GTIFile and there it will detect the sources which the SIMPUT contains.

Now we know everything to perform a simulation for eROSITA. But then again the simulation alone is not enough. The next step is to analyze it. Therefore we need the eSASS software.

## 3.2. eSASS

To analyse the performed simulations the software eSASS (extended Science Analysis Software System) is necessary. Since the software is still under development I used the user release version `eSASSusers_161130`. I will give a short



explanation of the different task I used of eSASS, although not all of them have a reasonably complete description yet.<sup>6</sup>

**evtool:** It merges multiple input eROSITA event FITS files, which are the output of SIXTE's erolim, into a single file.

**expmap:** This task computes exposure maps of one or several eROSITA telescopes for the all sky survey or pointed observations.

**ermask:** No description available. The result of this task is the creation of a detection mask.

**erbox\_local:** No description available. The outcome is a local box detection source list. In that list all significant sources are listed. A source is significant if it is within the sigma distribution of the background with Poisson calculation. Knowing the size of each detector the background is predictable.

**erbackmap:** No description available. To each energy band there will be a creation of a background image and a cheesemask, which is an image in which all sources were cut out.

**erbox\_m:** No description available. This one leads to a file called BoxDet-SourceListM and is similar to the one of erbox\_local.

**ermldet:** This task performs a maximum likelihood detection. It determines source parameters like positions, count rates, and source extent. This is done by fitting the PSF to the relevant region of the input science images for each source provided in an input source list. ermldet delivers a source list and optional source model maps as data products.

**catprep:** The catalog preparation tool is used for conversion, more precisely to convert the output file of the ermldet task into a catalog source list. If no unique match of a source is found in the cumulative source lists, a unique source name will be given. Furthermore matching sources can be written into a FITS file. The cumulative lists can be updated with new sources in pipeline processing.

There is also another task called srctool which is not yet operational. It will produce for each source and for each instrument one of the following file types: Spectrum, light curve, RMF, ARF, Event file and a source GTI extension.

---

<sup>6</sup>The webpage containing this information is only accessible for members <https://wiki.mpe.mpg.de/eRosita/eSASS>



## 4. Simulation

Now that we know how the software works we are able to perform the simulations for eROSITA. As mentioned in Sec. 1.2, eROSITA is going to perform an all sky survey in the first four years of its mission and after that a pointed observation for about three years. My simulations for the all sky survey build on each other. I have begun to create a region in the sky, a so called skymap, near the ecliptic pole. Then I have added step by step further information to that skymap. For a simulation to be as real as possible it is necessary to feed the software with as many data as available. But let us start with a simple example of a simulation with only one source. There are also some parameters that have not been changed during the simulations and can therefore be explained in more detail.

### 4.1. Simple example

In Sec. 3.1.2, I gave a quick overview of the different parameters which the SIXTE tool `erosim` requires (XMLFile, Attitude, (RA and Dec), Simput, MJ-DREF, (Exposure) and GTIFile).

The XMLFile, which contains the ARF, RMF, PSF and vignetting files, is defining the instrument and therefore not really changed, but later on just added by one more data. The files used for the above-mentioned functions in the same order are

- `erosita_iv_1telonaxis_ff.arf`
- `erosita_iv_1telonaxis_ff.rmf`
- `erosita_psf_v2.1.fits`
- `erosita_vignetting_v2.1.fits`

and all of them are listed in each `erosita_1-7.xml`, as there are seven telescope modules and each one has an own XMLFile.



For the attitude, the file named `att2_4yr_1min_keys_fix.fits` was used. Due to eROSITA's scanning method the complete sky will be scanned eight times, thus one scan will take half a year. Using the attitude, `erosim` starts the simulations with 0 sec and  $RA = 90.40^\circ$  and  $Dec = 23.44^\circ$ . With increasing time eROSITA will look at different regions in the sky. The attitude ends after 126230400 sec, corresponding to four years in seconds, with  $RA = 90.40^\circ$  and  $Dec = 23.44^\circ$ . The attitude file has a time resolution of 60 sec, i.e., it has 2103840 entries. The total exposure is therefore 126230400 sec.

The SIMPUT file is the only data that changed during the simulations, apart from the XMLFile where just a further information was added. Actually I just added more SIMPUT files containing other data. For the eROSITA all sky survey the `rass.simput` was used as the basic framework (the abbreviation RASS stands for ROSAT all sky survey). It is the result of the previous ROSAT mission and contains 124731 sources in the X-ray (Voges et al., 1999). For the simple example seen in Fig. 4.1 the `crab_radec.fits` was used. It contains only one source at  $RA = 90.35$  and  $Dec = 0.0$  with an original flux of  $2.052122 \cdot 10^{-10}$  erg s<sup>-1</sup> cm<sup>-2</sup>. For a better result I changed it to  $2.052122 \cdot 10^{-8}$  erg s<sup>-1</sup> cm<sup>-2</sup>. The unit erg s<sup>-1</sup> cm<sup>-2</sup> is common in X-ray astronomy with

$$1 \text{ erg} = 10^{-7} \text{ J} \approx 6.28 \cdot 10^8 \text{ keV}$$

MJDREF is a fixed value as mentioned in Sec. 3.1.2. In the event list each detected photon is listed with its position and its time relative to MJDREF. Adding to that time the MJDREF the correct determination of the photon detection is possible, which means the concrete day and time can be calculated.

The value of the exposure is the time a simulation lasts. In combination with the attitude this means that after the given exposure the simulation stops. If you want to simulate a specific region in the sky, as I did, you either define your exposure with a START and STOP time or with a GTIFile. I used the GTIFile `gti1_new.fits`, which is actually just a list with all START and STOP times of the sources in the created skymap. This means that in combination with the attitude eROSITA will only observe the sources, that are in the FOV during the given times in the GTIFile.

Fig. 4.1 shows the difference of a simulation for a telescope for the slew survey (left) and for a pointed observation (right). As mentioned above, without the

# Simulations for eROSITA:

First impressions on the imaging properties



## 4. Simulation

---

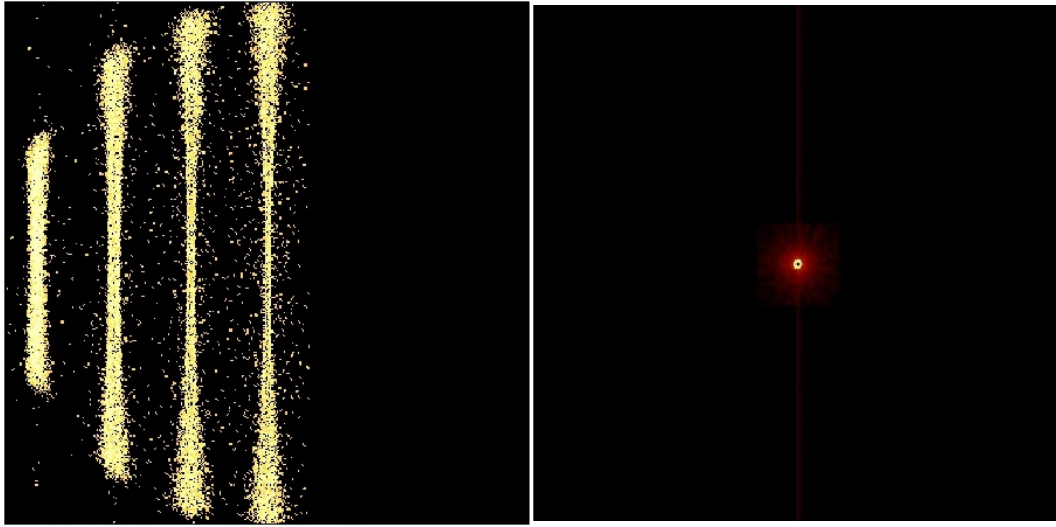


Figure 4.1.: Focal plane image of the simulation of one source with an exposure of 57600 sec

Left: Due to the attitude eROSITA is rotating around its axis. That way a slew is emerged. Four slews are seen, since one revolution takes 14400 sec

Right: A pointed observation is seen here. Pile up, the PSF and the readout process can be seen clearly

attitude eROSITA will only observe the location defined by the RA and Dec coordinates during the given exposure (right picture). Due to the higher flux, the source is much brighter. This way pile up, the PSF, and the readout process can be seen more clearly. Pile up, as mentioned in Sec. 2.2, occurs when a source is too bright. That way, the detector is not able to distinguish whether the detected energy is from one photon or the sum of more photons. The weak streak going through the right picture leads back to the readout process, where the data is shifted through every pixel to be read out. The PSF is the reason why the source in the right picture is smeared. The higher the energy of a photon the more it will blur. Especially on the left picture the PSF is obvious, since it is not only depending on the photons energy but also on the off-axis angle and the azimuthal angle. This is why the slews on the boundaries of the FOV are much more blurred than in the center.



## 4.2. Creating the Skymap

The skymap I created is near the ecliptic pole locating at  $RA = 93.461538^\circ$  and  $Dec = -66.018281^\circ$ . This region was chosen for the simulations because of the higher exposure available at the ecliptic poles. In that way eROSITA's sensitivity will be tested, due to a detection of more photons. Apart from the SIMPUT, I used the `rass.simput`, the first simulation was run with the parameters as described in Sec. 4.1.

In order to get the simulations as realistic as possible, the `rass.simput` alone does not contain enough information. In the sky there are more than just the sources in that catalog for that specific region. For this reason, more data were added. The file called `agnlist_skymap93156_above2e-16.fits.gz` is the first dataset made by Clerc (2014). This file contains data of a simulated AGN population. The AGNs are randomly distributed across the field. Their spectra are modelled following Gilli et al. (2007). This file is used as a second SIMPUT for the simulations. The second one is `bkg_lc_1.fits.gz`, also made by Clerc (2014). This file simulates the particle and galactic background as many new faint sources. As mention above, X-ray detectors are also sensitive to ionized particles other than X-rays. This is the file that was added to each XMLFile. The development of the simulation can be seen in Figs. 4.2, 4.3 and 4.4.

It is nice to see the evolution of the simulations. The brighter spot in the right corner is the ecliptic pole. Since it gets more exposure, it appears brighter compared to the rest. The first simulation looks a little bit too artificial, because there are only the sources to be seen that are in the `rass.simput`. By adding more data into the simulation the figures get more and more real. By this I mean that with detecting more photons by eROSITA the simulations are more reliable to the reality. The detectors do not only register the photons emitted from the observed sources but also the background emission. And since it is predicted that eROSITA will detect 50000 to 100000 new galaxy clusters, let us fake some new sources to the skymap.





4. *Simulation*

---

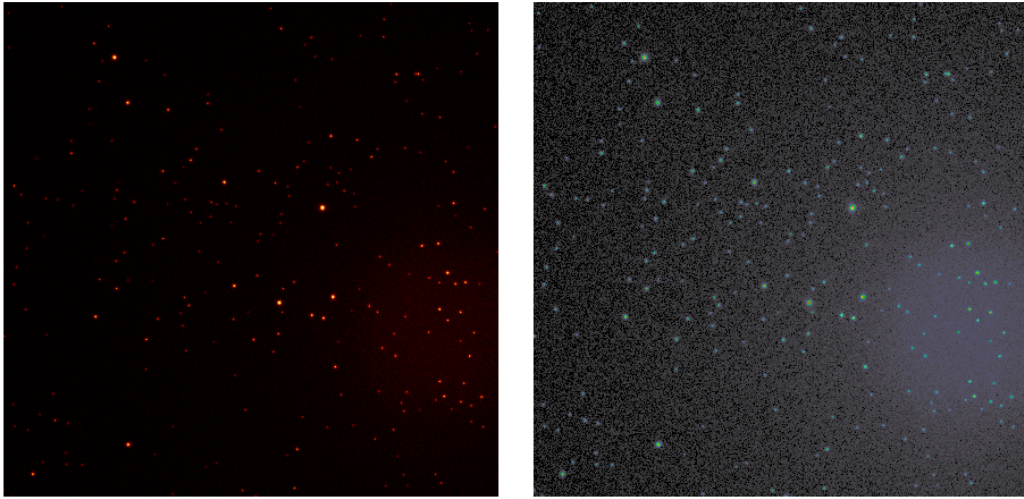


Figure 4.2.: This is the first simulation, containing only the RASS sources. Both figures are the same, only with a different colouring

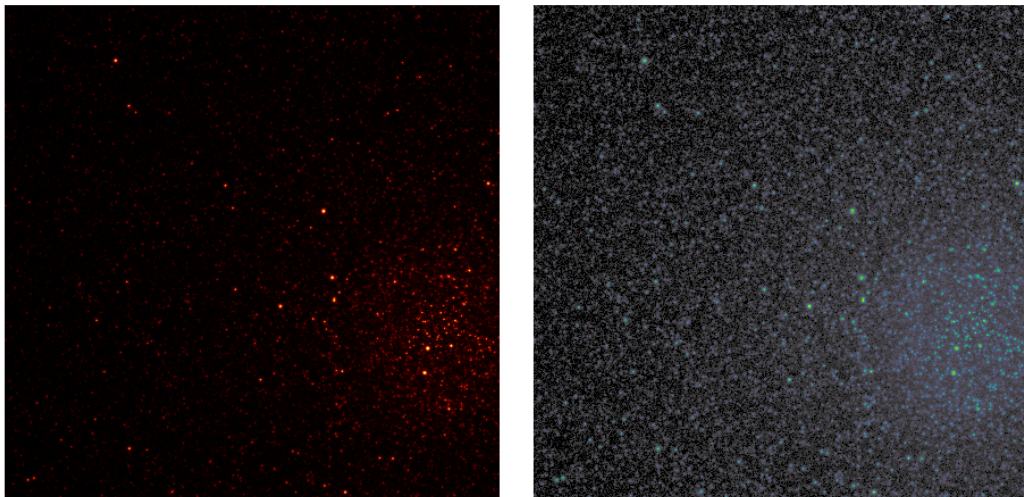


Figure 4.3.: Second simulation to which the AGN population was added

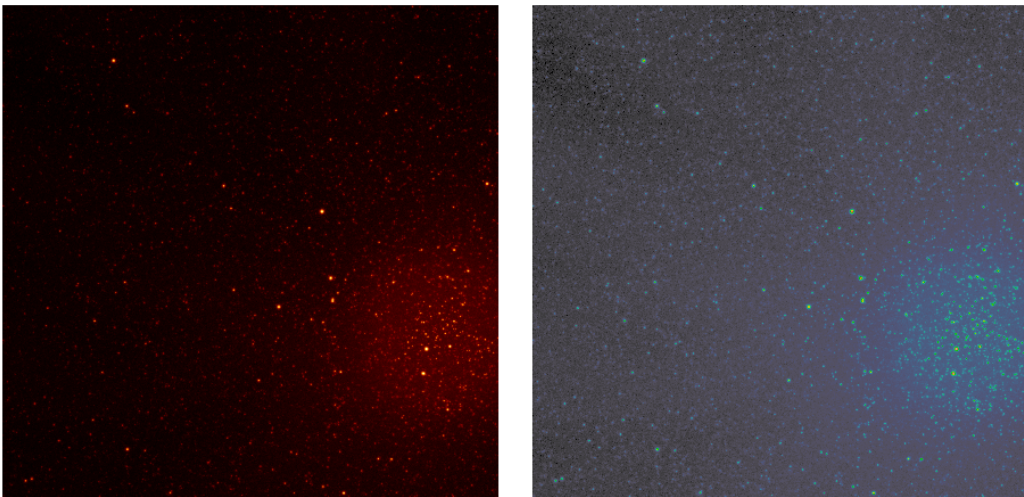


Figure 4.4.: Third simulation with additional variable sources



### 4.3. Andromeda Galaxy aka M31

The Andromeda Galaxy, also known as Messier 31 (M31), is the nearest galaxy to the Milky Way Galaxy where we live in. It is a spiral galaxy located “only” 2.5 billion light years away. Since it is our neighbour it seems obvious to study it. This is the reason why we know for example that there are 26 black hole candidates or that in several billion years from now our galaxy and Andromeda will collide (NASA, 2013).

#### 4.3.1. Simput of M31

Since there was no SIMPUT file of M31 I created one with data gathered with XMM-Newton. The XMM-Newton (X-ray Multi-Mirror Newton) is another X-ray satellite. It was launched on 18.12.1999 with a mission extension to at least 31.12.2018 due to its successful mission. During the time of June 2000 to July 2004 and June 2006 to February 2008, XMM-Newton observed M31 resulting in a source list of 1948 detected sources with 914 detections for the first time (Stiele et al., 2011).<sup>7</sup>

The position, the name and the flux of each source was given in that list. For  $E_{\min}$  and  $E_{\max}$  I used the borders of eROSITA, 0.2 keV and 10 keV. Assuming that the fluxes do not vary with time but are constant there was no need for TIMING. So only the SPECTRUM had to be created.

For the spectrum a simplification was assumed, meaning that each source has the same spectrum. It can be described as a product of a power law with a factor which is considering the absorption of the interstellar medium (Wilms et al., 2000). The power law is a special shape defined as

$$A(E) = K \cdot E^{-\alpha} \quad (4.1)$$

with  $K = 1$  being a norm factor and  $\alpha = 2$  is the photon index which was set to 2, as this is a realistic value (Wilms et al., 2000). The absorption, which is given by

$$I_{\text{obs}}(E) = e^{-\sigma_{\text{ISM}}(E) \cdot N_{\text{H}}} \cdot I_{\text{source}}(E) \quad (4.2)$$

---

<sup>7</sup>In the article they talk about 1897 sources, later the number was updated <http://adsabs.harvard.edu/abs/2011yCat...35340055S>

## Simulations for eROSITA:

First impressions on the imaging properties



### 4. Simulation

---

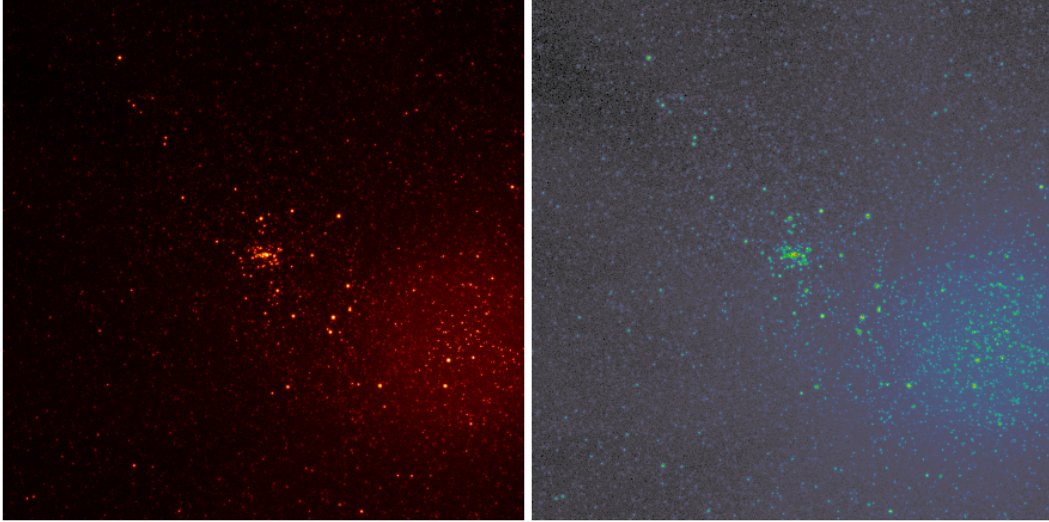


Figure 4.5.: Fourth simulation with RASS, AGN population, variable sources and now additional with M31

was set to 0.01.  $I_{\text{obs}}(E)$  is the observed X-ray spectrum of a source,  $I_{\text{source}}(E)$  is the emitted X-ray spectrum,  $\sigma_{\text{ISM}}(E)$  is the sum of photo ionization cross sections and  $N_{\text{H}}$  is the hydrogen equivalent column along the line of sight measured in atoms/cm<sup>2</sup>.

The result was a SIMPUT file containing 1948 sources. The only problem was that its original RA and Dec coordinates were different from the ones of my skymap. That could easily be solved by rotating M31 into the skymap. Therefore I just used a function to rotate the input file (M31) with its original RA and Dec positions to the desired RA and Dec coordinates. After that the new SIMPUT was added to the simulations, seen in Fig. 4.5. The bright spots in the middle of the pictures are the center of the Andromeda Galaxy.

#### 4.3.2. Diffuse emission of M31

Just like before, the sources alone are not enough for a realistic simulation. So the next step was to add a diffuse emission of M31. Therefore I used data of XMM-Newton again. This time not a list with sources, but a finished picture of the Andromeda Galaxy provided by Manami Sasaki. Due to the size of M31 with almost 220 000 light years across, the galaxy can not be depicted in a single figure but consists of many parts. In other words the picture of M31 which is used was a mosaic picture, seen in Fig. 4.6. Looking closely one can



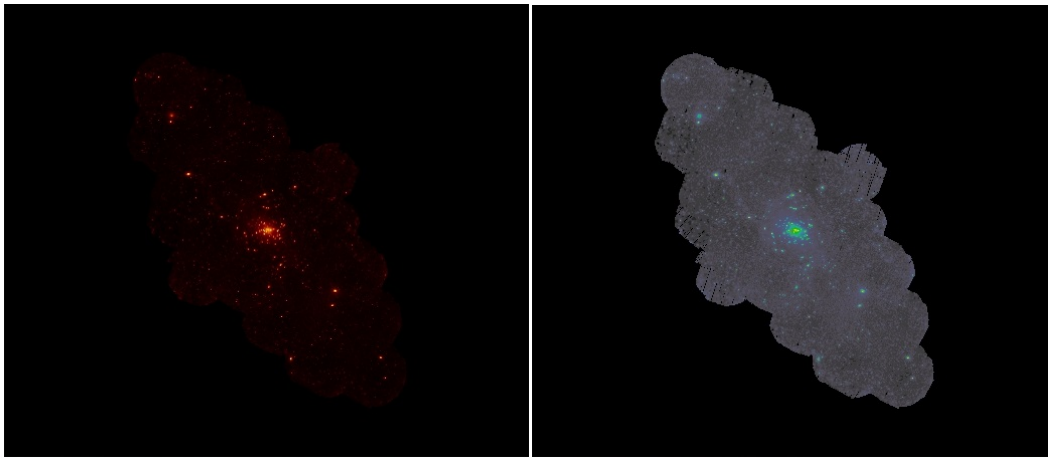


Figure 4.6.: The mosaic picture of the Andromeda Galaxy taken by XMM-Newton

see that it was composed of individual pictures. For the diffuse emission, I had to cut out the sources of the mosaic picture, so that only the faint background would be left. Since I now had a SIMPUT with all the sources, I just had to get rid of them in the mosaic. Therefore I marked all sources in the mosaic by comparing the positions of each source, both the sources in the mosaic as well as in the SIMPUT. After that I defined the size of the circle to cut each source  $r$  by using Pythagorean theorem. For a source with position  $X$  and  $Y$  it is

$$(X, Y) = \sqrt{\left(X - \frac{r}{\sqrt{2}}\right)^2, \left(Y - \frac{r}{\sqrt{2}}\right)^2} \quad (4.3)$$

I defined three sizes of circles. Therefore I changed  $r$ , because of the different fluxes of the sources which make the wings of the PSF more apparent for multiple sources. A brighter source will be cut out with a bigger circle and thus a fainter source with a smaller one. The result was a mosaic picture of M31 where all source were cut out which can be seen in Fig 4.7. Now all what was left to do, was to fill these holes with information. I excluded the brighter regions of my calculations and then formed the mean value of what was left. In the center there was a brighter background due to pile up of higher fluxes of the sources that would have compromised my assumption. With that mean value I filled the holes to get the diffuse emission of the Andromeda Galaxy (Fig. 4.8). Now the holes are filled with data and the figure can be used as the diffused emission of the Andromeda Galaxy by adding it to the SIMPUT. The outcome of that simulation can be seen in Fig. 4.9. The circle that is clearly



4. *Simulation*

---

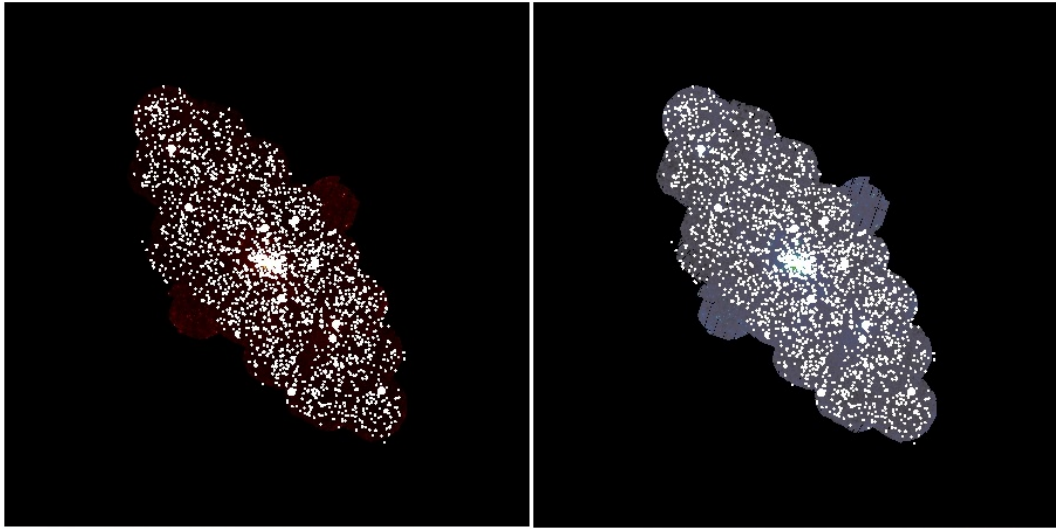


Figure 4.7.: All sources of the SIMPUT are cut out and holes in the mosaic are the result

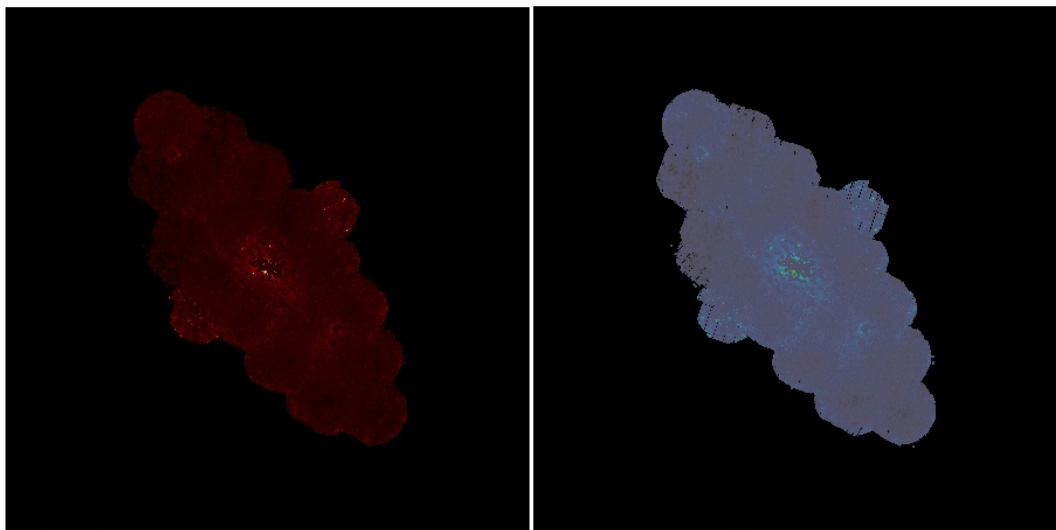


Figure 4.8.: The holes in the mosaic are now filled with some data in order to create a diffuse emission of M31

seen shows the diffuse emission of the Andromeda Galaxy. The few sources outside of that circle are from the RASS.

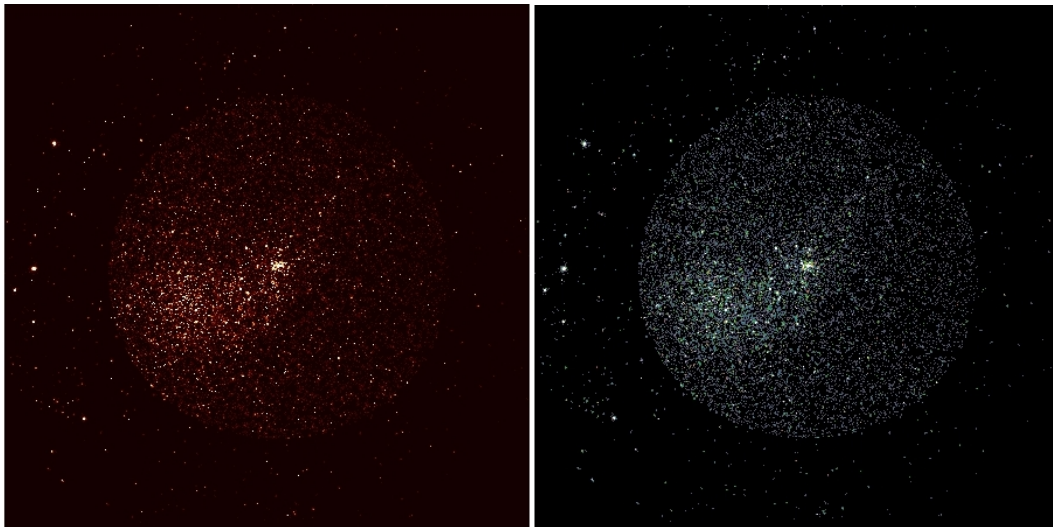


Figure 4.9.: This is a picture showing the diffuse emission of M31 together with all the other parameters

## 4.4. Analysing the Skymap

The big advantage of SIXTE is its usage for different instrument missions. The output is always neutral and therefore has to be converted for the specific instrument. This is why the seven created event lists were first converted by the function `ero_calevents`. After that the files had the necessary format eROSITA uses. Then the `evtool` was used to merge the seven event files into one and creating an image of that. The picture seen above in this chapter are the result of that `evtool`. Last but not least, before starting with eSASS, the RA and Dec coordinates had to be converted for the analysis into X- and Y-Pixel positions. I will concentrate on the fourth simulation and analysis, since the software is yet not able to analyse the diffuse emission. The different tasks of eSASS I used to analyse the simulations are mentioned in Sec. 3.2. The precise order of the task is important, as they build on each other. The first one is `evtool`. Since the seven event files of `erosim` are already merged into a single file, it filters the four different energy bands of that single file and thus creating four new event lists. Now it is possible to reconstruct how many photons have been detected in the corresponding energy band. It seems logical that with increasing energy more photons are detectable, especially at the ecliptic pole which has the highest exposure (Fig. 4.10 and 4.11). Appendix A.1 shows the same figures with different colouring. After that, `expmap` follows. It generates of each energy band an exposure map for each telescope module. It contains the START and STOP

## Simulations for eROSITA:

First impressions on the imaging properties



### 4. Simulation

---

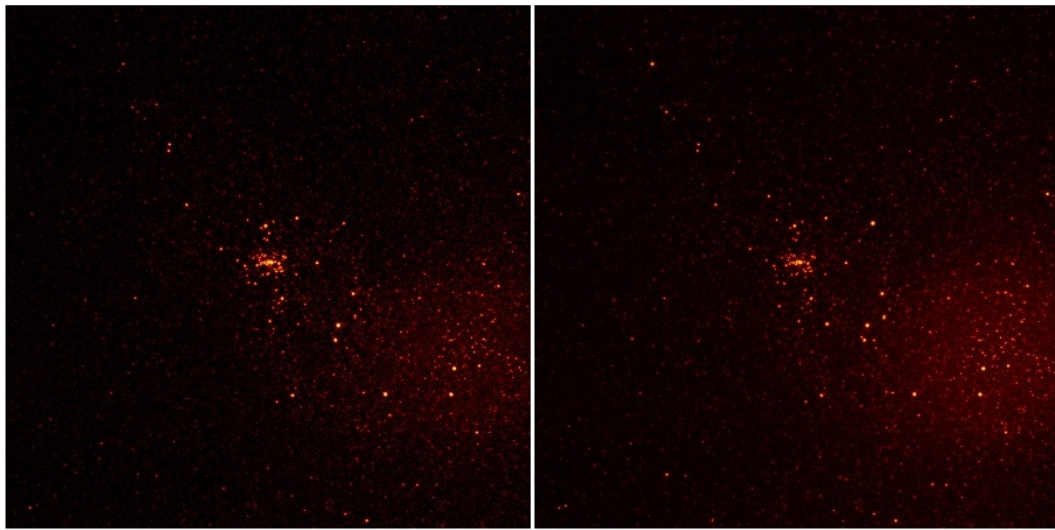


Figure 4.10.: On the left there is the energy band 1 (0.2 - 0.5 keV). On the right is the second one (0.5 - 2 keV). The increasing brightness at the ecliptic pole is clearly visible

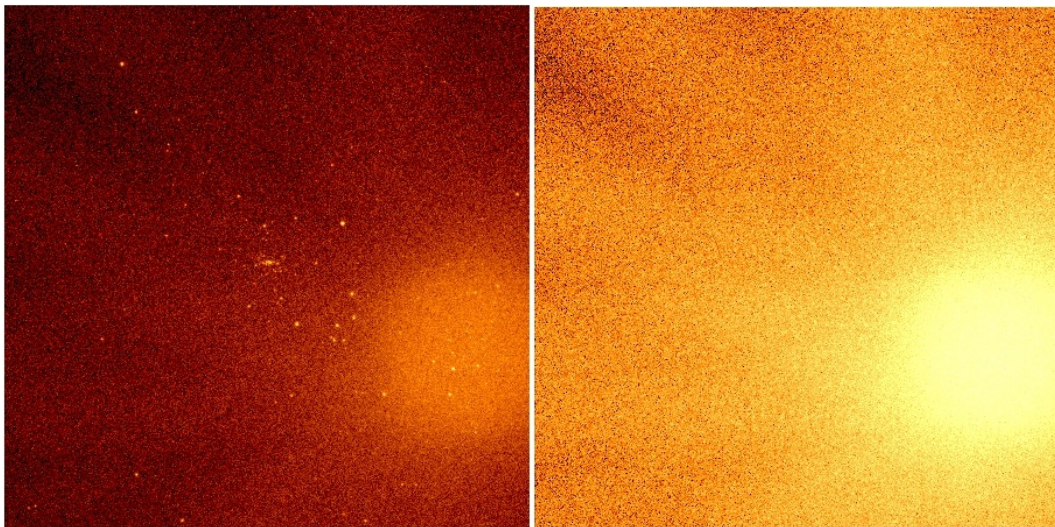


Figure 4.11.: Due to the high exposure of the ecliptic pole it is hard to see other sources in the third (2 - 5 keV) and fourth (5 - 10 keV) energy band

times of the detected photons for the specific telescope and corresponding energy band, or in other words it creates the GTIFiles. Of these exposure maps, `ermask` calculates the detection mask which is independent of the energy bands. This detection mask is actually just a table with the value of 1, which means that every pixel of each telescope was able to detect the incoming photons. The next task is `erbox_local`. It uses the output of the `evtool` with the four





## Simulations for eROSITA: First impressions on the imaging properties

### *4. Simulation*

---

energy bands and creates a local boxlist containing a source list. The output of erbackmap are cheesemasks and background images to each energy band. As input, it requires the out files of evtool with the four energy bands. A cheesemask is just a figure without sources, similar to the file I created for the diffuse emission of M31 by cutting out all sources. The background image is exactly what the name suggests. erbox\_m is similar to erbox\_local and is generating another source list. The maximum likelihood detection ermldet is creating to each evtool output file a corresponding source list where every photon is listed. Additionally another source list file is generated. Last but not least, catprep is preparing the catalog for the srctool. The result is one file containing all sources of all four energy bands.





## 5. Results

After completing the simulations and running the analysis software it is now time to have a look at the results. Here again I will concentrate on the fourth simulation because I have not enough data on the one with the diffuse emission of M31 which is the fifth simulation.

The results of the simulations done with *erosim*, a *SIXTE* tool, have already been shown in Sec. 4.2 and 4.3.1, to be seen in Figs. 4.2 to 4.5. It is clearly to be seen that with increasing data the outcome of a simulation differs. This correlation is also to be seen in the merged event files of each simulation. The more data I used for one simulation the more events were listed in the files.

However I noticed a strange difference between the third and fourth simulation. Comparing their merged files, the third simulation has more events in its list than the fourth one. Although the fourth simulation contains data of the RASS, AGN population, various sources and the Andromeda Galaxy it has about 690000 events less than the third one which is a simulation without the M31. Taking a closer look in the fourth simulation there are 20% more photons simulated than in the third one. But since in the event list of the fourth simulation there are less events listed, it means that there are more invalid events. Invalid events are events that are not listed in the event lists. Perhaps this can be explained by pile up. With M31 in the simulation there are more bright sources and therefore more possible pile ups. As explained before if pile up occurs the detector is not able to distinguish if a detected energy is the sum a few photons or just a single one. So eventually the same thing happened here. Emitted photons of a source at location X and Y are detected due to their high energy. From the same position fainter photons are detected too, but they will not be recognized as an individual source but are accredited to the high energy source.

Although I do have now a picture of the next simulation with the diffuse emission of M31 (Fig. 4.9), I am not able to analyse it because the software

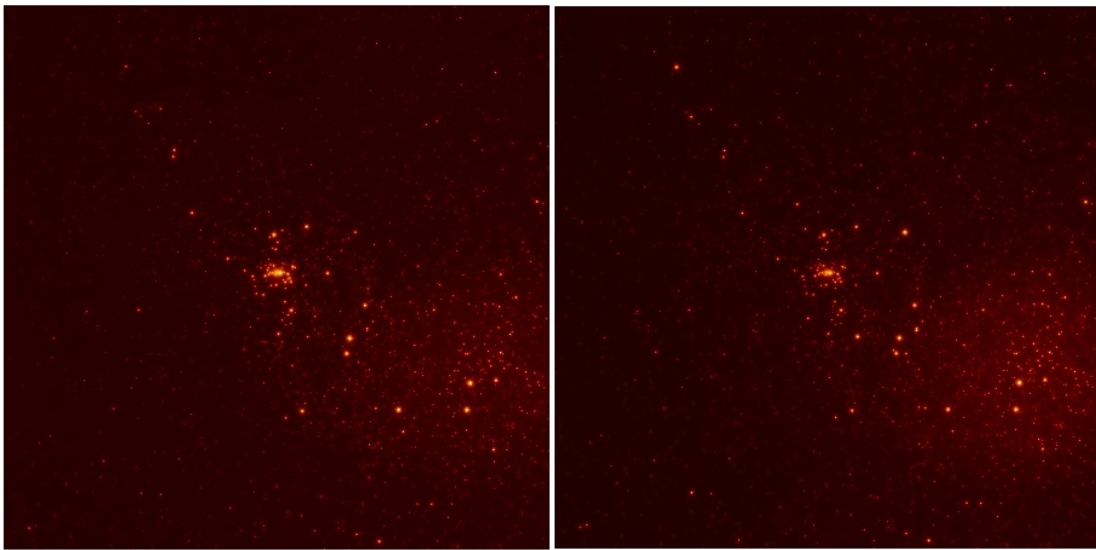


Figure 5.1.: On the left there is the source map of the energy band 1 (0.2–0.5 keV). On the right is the second map of the second energy band (0.5–2 keV)

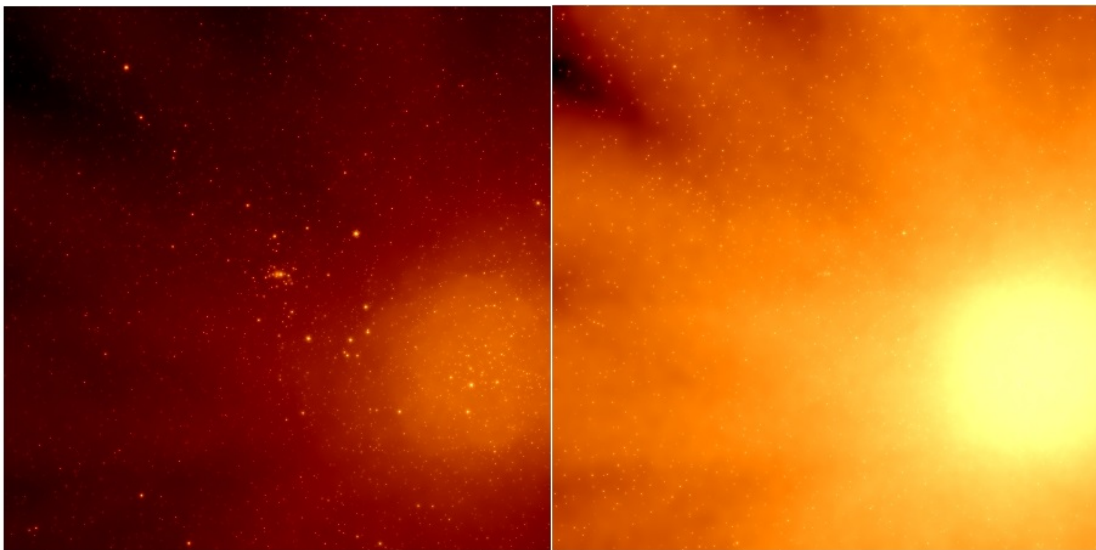


Figure 5.2.: Although the exposure is high at the ecliptic pole the some sources can be seen

is still under development. It would have been nice to see how the simulation would look like in the different energy bands, how their source maps would look like, and how many sources would have been detected in the source catalog.

In Sec. 4.4, I showed the four different energy bands. The sources in these figures could not be seen very well. But thanks to `ermlDET`, which creates a source map of each energy band, one is able to detect them. Even in the higher

## Simulations for eROSITA:

First impressions on the imaging properties



### *5. Results*

---

energy bands (2–10 keV) the sources can be detected in the source map, in contrast to the figures seen in Sec. 4.4, where this was only possible in the first (0.2–0.5 keV) and second energy band (0.5–2 keV). In appendix A.2 there are the same pictures again, but with another colouring.

Since there is no `ero_archive` yet I can not confirm that `catprep` is working properly. `catprep` should write unique source names to each file for which no unique match is found in cumulative lists of sources in the `ero_archive`. But as just said there is no archive yet. That means that every detected source is listed in that source catalog. For my first simulation 454 entries are listed in the source catalog which seems realistic. For the second there are 7452, for the third and fourth there are 6033 entries. One might think that this result is wrong, but it is probably not. In the third simulation there was the background light curve added with the various sources. That will make it harder for too faint sources to be detected which leads to a decreasing number in the source catalog.

Since the eSASS software is still in development I am not able to tell if the `srctool` works properly, because I could not test it.



## 6. Conclusion

As mentioned before SIXTE, more precisely erosim, is the software to perform the simulations. So it would be interesting to know how much data the software can handle and where the borders are in order to still get a realistic simulation. Apart from this pile up is problematic. If some source are too bright the detection will not work correctly. In that case a defined border for pile up would help. A message could be given if in a specific region pile up occurred. Subsequently that region could be observed more carefully to make sure if there are more sources in that location, but weaker ones. In that way the discovery of new sources could be made easier.

In the next step the simulation with the diffuse emission of M31 should be analysed. After that the results should be compared with the previous simulations. Especially since there might be a problem with invalid events. Although a larger number of photons was simulated, too few were detected. Furthermore ULXs (ultra-luminous X-ray sources) should also be simulated in order to test eROSITA's imaging properties. A ULX is a very bright X-ray source that is common in many galaxies. It would be interesting to see how such a source would look like and if or how pile up would influence the simulation.

In my thesis I concentrate on a region near the ecliptic pole to get an impression on the imaging properties of eROSITA, due to the high exposure in that region. In addition to that a simulation should also be performed at the equator where there is less exposure. None the less the simulations that are shown in this thesis are great examples of what can be performed and analysed.



## Bibliography

- Aschenbach B., 1985, Reports on Progress in Physics 48, 579
- Aschenbach B., 2009, Experimental Astronomy, Vol. 26, Ch. Realization of X-ray telescopes—from design to performance, p.951
- Brand T., Dauser T., Peille P., Wilms J., 2016, SIXTE Manual available at [http://www.sternwarte.uni-erlangen.de/research/sixte/data/simulator\\_manual\\_v1.1.pdf](http://www.sternwarte.uni-erlangen.de/research/sixte/data/simulator_manual_v1.1.pdf)
- Calabretta M.R., Greisen E.W., 2002, A&A 395, 1077
- Clerc N., 2014, Description of Release\_July2014
- George I., Arnaud K., Pence B., et al., 2007, The calibration requirements for spectral analysis, available at [ftp://legacy.gsfc.nasa.gov/caldb/docs/memos/cal\\_gen\\_92\\_002/cal\\_gen\\_92\\_002.pdf](ftp://legacy.gsfc.nasa.gov/caldb/docs/memos/cal_gen_92_002/cal_gen_92_002.pdf)
- Gilli R., Comastri A., Hasinger G., 2007, A&A 463, 79
- Grossberger C., 2014, New developments and techniques in radio to X-ray observations of AGN, PhD thesis, Friedrich-Alexander University of Erlangen-Nuremberg
- Hanisch R.J., Farris A., Greisen E.W., et al., 2001, A&A 376, 359
- Kartunen H., Kroeger P., Oja H., et al., 2003, Fundamental Astronomy, Springer, Berlin, Heidelberg
- Lumb D., Berthiaume G., Burrows D., et al., 1991, Experimental Astronomy, Vol. 2, Ch. Charge coupled devices (CCDs) in X-ray astronomy, p.179
- Meidinger N., Andritschke R., Ebermayer S., et al., 2009, UV, X-Ray, and Gamma-Ray Space Instrumentation for Astronomy XVI, 1
- Merloni A., Predehl P., Becker W., et al., 2012, eROSITA Science Book: Mapping the Structure of the Energetic Universe



- NASA 2013, Andromeda Galaxy, available at [https://www.nasa.gov/mission\\_pages/chandra/multimedia/bonanza\\_image.html](https://www.nasa.gov/mission_pages/chandra/multimedia/bonanza_image.html)
- Pence W.D., Chiappetti L., Page C.G., et al., 2010, A&A 524, 40
- Predehl P., 2010, The Platinum Age, Presentation at Erhard-Karls Universität Tübingen
- Schmid C., 2012, X-ray Telescopes in the Digital Lab: Instrument Performance Simulations, PhD thesis, Friedrich-Alexander University of Erlangen-Nuremberg
- Schmid C., Smith R., Wilms J., 2013, SIMPUT available at <http://hea-www.harvard.edu/heasarc/formats/simput-1.1.0.pdf>
- Seward F.D., Charles P.A., 2010, Exploring the X-ray Universe, Cambridge University Press, Cambridge
- Stiele H., Pietsch W., Haberl F., et al., 2011, A&A 534, 51
- Trümper J.E., Hasinger G., 2008, The Universe in X-ray, Ch. Wolter Optics, p.41, Springer, Berlin, Heidelberg
- Voges B., Aschenbach B., Boller T., et al., 1999, A&A 349, 389
- Wille M., 2011, Detector Performance of eROSITA, Friedrich-Alexander University of Erlangen-Nuremberg
- Wilms J., 2017, X-ray astronomy, available at <http://hydrus.sternwarte.uni-erlangen.de/~wilms/teach/xray2012/chapter0004.html>
- Wilms J., Allen A., McCray R., 2000, The Astrophysical Journal 542, 914
- Wolter H., 1952, Annalen der Physik 445, 94



## Acknowledgements

First of all I like to thank my supervisor at the observatory Jörn Wilms for this great opportunity. Since I was a toddler I was interested in astronomy. Writing my bachelor thesis at an observatory and performing simulations for an X-ray satellite which will be launched soon was awesome.

Special thanks to Thomas Dauser for introducing me to SIXTE and answering my questions (sometimes even stupid ones) concerning this topic. A big thank you goes to Christoph Grossberger for explaining and helping me with the eSASS software. Without him I would have been hopelessly lost. He was always patient with me and pushed me in the right direction.

I also want to thank my co-workers in the office Ralf Ballhausen, Thorsten Brand, Florian Erbesdobler, Tobias Hain and Shu Niu for the delightful conversations, a box full of sweets and fun. Actually I want to thank everybody at the observatory for the great time.

Last but not least, I would like to thank my family and friends for enduring my spontaneous emotional changing moods in the last two weeks and for still talking to me.



## Eidesstattliche Erklärung

Ich, Margarita Behm, Matrikel-Nr. 00473513, versichere hiermit, dass ich meine Bachelorarbeit mit dem Thema

*Simulations for eROSITA: First impressions on the imaging properties*

selbständig verfasst und keine anderen als die angegebenen Quellen und Hilfsmittel benutzt habe, wobei ich alle wörtlichen und sinngemäßen Zitate als solche gekennzeichnet habe. Die Arbeit wurde bisher keiner anderen Prüfungsbehörde vorgelegt und auch nicht veröffentlicht.

Lichtenfels, 8. März 2017

---

MARGARITA BEHM





## A. Appendix

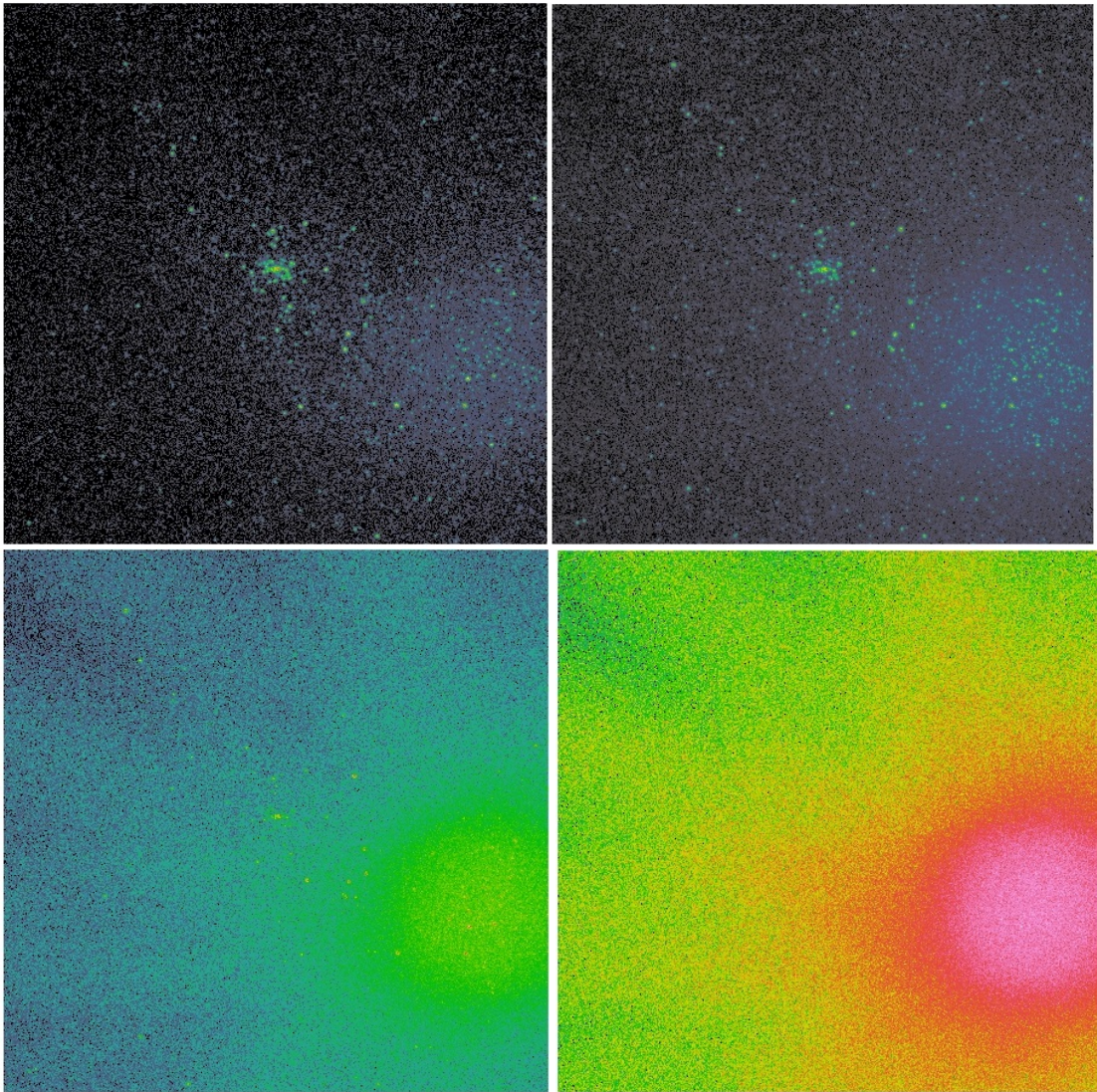


Figure A.1.: The four different energy bands with increasing energy from upper left to bottom right with different colouring

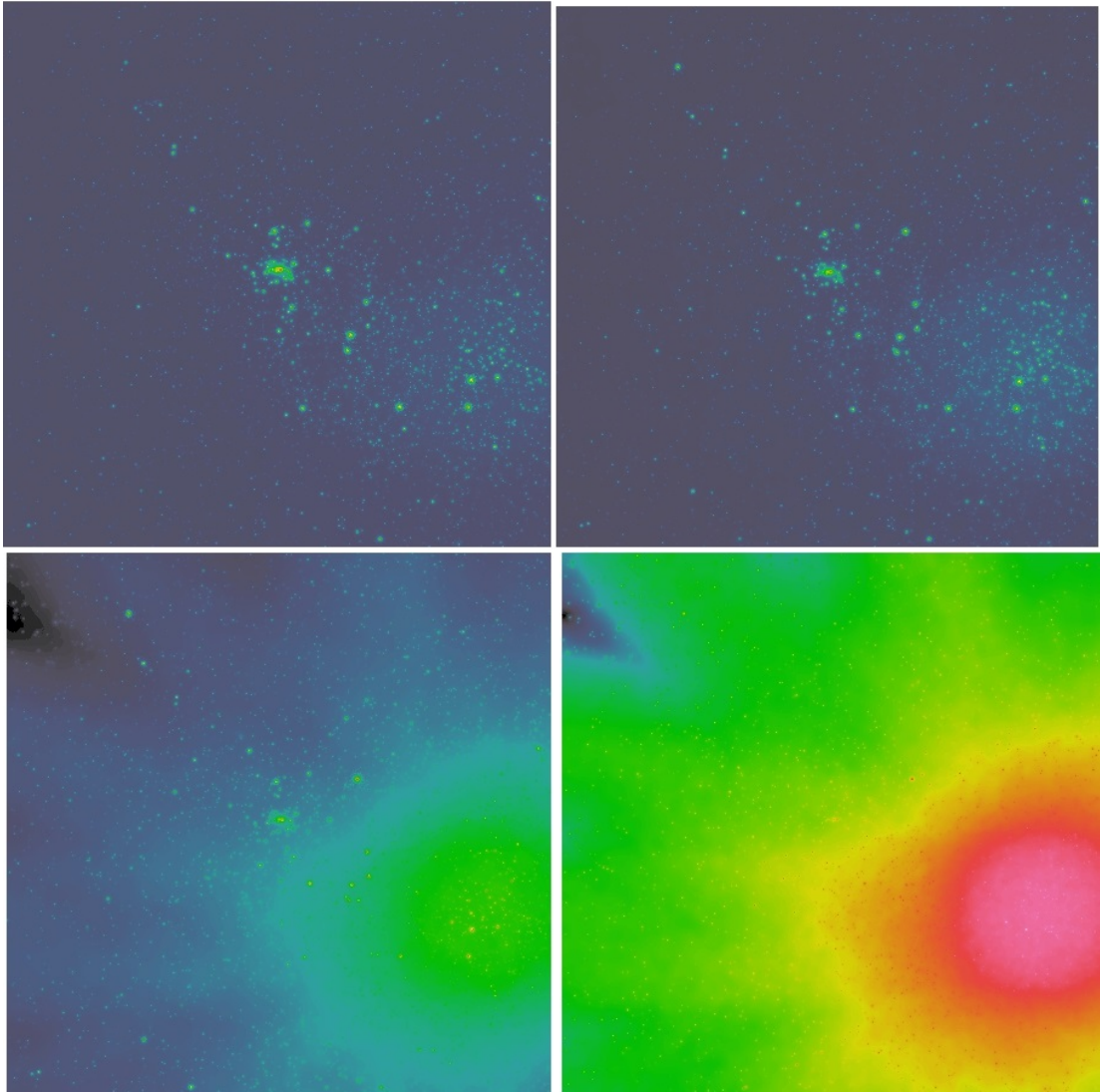


Figure A.2.: Unfortunately due to the colouring it is hard to see the sources in the higher energy bands. In the other colour (Fig. 5.1 and 5.2) it is way easier